© creative

Scientific paper

Elimination of Cadmium using Silica Gel Prepared from Blast Furnace Slag

Toufik Chouchane^{1,*}, Mohamed Tayeb. Abedghars ¹, Sabiha. Chouchane² and Atmane Boukari¹

¹ Research Center in Industrial Technologies CRTI, P.O. Box 64, Cheraga 16014 Algiers Algeria

² Faculty of Sciences, Badji Mokhtar University, Annaba Algeria

* Corresponding author: E-mail: chouchane_toufik@yahoo.fr t.chouchane@crti.dz

Received: 02-13-2024

Abstract

In this work, the silica gel recovered from the blast furnace slag was exploited for the elimination of cadmium in batch mode under the action of different factors. Physico-chemical analyzes revealed that the modified slag is only composed of silica (96.14%). Its specific surface area is $484 \text{ m}^2\text{g}^{-1}$ and the pH corresponding to point of zero charge is 4.2. Adsorption isotherms demonstrated that the removal of cadmium on modified slag The experiment revealed that at pH 6, the effect of the determining factors contributed to the progression of the sorption capacity, which was measured at 154.11 mg/g and was accomplished on a homogeneous monolayer surface ($R^2 = 099$). Kinetic analysis revealed that this process agreed with the pseudo-second-order kinetic model ($R^2 \ge 0.99$). In addition, it was indicated that the diffusion of the pollutant is ensured by external and intraparticle diffusion. The values of thermodynamic variables clarified that cadmium sorption is spontaneous, exothermic, less entropic and physically executed under the effect of electrostatic interaction. The desorption process revealed that the reuse of Silica gel was feasible over five consecutive cycles.

Keywords. Adsorption, Cadmium, Isotherm, Kinetics, slag, Silica gel

1. Introduction

Water contamination has become a major global problem, with its effects on humans and their environment. Indeed, used oils, organic materials (dioxins, polychlorinated biphenyls, polycyclic aromatic hydrocarbons, pesticides, etc.), and especially toxic metals (Cd, Hg, As, Pb, Cr, Ni, Zn, Mn, etc..) are continually released into the environment, causing serious pollution of fauna and flora, which will directly or indirectly affect the economy and the health of populations. 1 To guarantee a healthy environment and preserve this natural wealth (water), it is necessary to impose severe sanctions against all forms of pollution. In addition, it is essential to use innovative technological processes, namely ion exchange, solvent extraction, reverse osmosis, ultrafiltration, microextraction of magnetic nanomaterials, and adsorption.² In the latter process, the use of inexpensive adsorbents such as natural materials and industrial solid waste have been widely indicated in recent times.^{3,4} In this context, we opted for research to

eliminate cadmium in solution by adsorption on silica gel prepared from blast furnace slag from the El Hadjar steel complex in Algeria.

Cadmium is widely used in several industries, namely mining, surface coating, the manufacturing of zinc, batteries, alloys, and solar cells. It is considered very harmful. Its accumulation in the organs represents the most dangerous action. Indeed, its introduction could cause hypertension, kidney failure, loss of calcium, reduction of red blood cells, and other harmful consequences.^{1,4} These effects have prompted the World Health Organization and the International Agency for Research on Cancer to classify it as an enormously harmful contaminant.⁵ From the literature, it was noted that the elimination of cadmium in solution had been the subject of multiple research studies. 6-15 It should be mentioned that the experimental results resulting from these applications displayed a good agreement and also an excellent affinity between the adsorbents examined and the cadmium ions in solution.

Blast furnace slag is a by-product regenerated during the production of cast iron from ores in steel blast furnaces. It is composed of lime, silica, alumina, magnesium oxide, and a small percentage of metal oxides.¹⁶ According to the bibliography, it has been cited that blast furnace slag was considered an adsorbent of choice for the removal of metal ions in solution. 16-20 From the literature, it has also been cited that various adsorbents were formulated from blast furnace slag. For example, blast furnace slag was transformed into hydroxyapatite-zeolite material for the adsorption of Mn²⁺, NH⁴⁺ and PO₄³⁻ ions, ²¹ and it was also successfully converted to slag oxalate for the adsorption of Co(II) ions in solution.²² Furthermore, the synthesis of silica nanoparticles from blast furnace slag was carried out in order to use them as an adsorbent to remove azo dyes,²³ and the Tobermorite hydrothermal was formulated from blast furnace slag for the adsorption of Cs+ and Sr²⁺.²⁴

Silica gel (SG) is a silicon hydroxide Si(OH)₄ polymer of silicic acid prepared from sodium silicate. Silica can be obtained by different extraction techniques, including the alkaline fusion method,²⁵ and the reflux extraction method.²⁶ According to research studies, the alkaline fusion method is the most effective due to its ability to decompose silica and alumina at high temperatures.^{27,28} The fusion of silica with alkali hydroxide is a key factor in the extraction of metals from solids.²⁹

Due to its high porosity and large specific surface area, silica gel has been exploited as an adsorbent in waters containing metal ions. ³⁰ Effectively, silica gel prepared from chemical waste bottles was used for the elimination of Zn(II) ions in solution. ³¹ The chemically modified silica gel with a thiol group has been suggested for the removal of toxic metals from industrial liquid discharges, ³² and modified with a chelating ligand has been proposed for the adsorption of mercury ions. ³³ Additionally, silica gel has been recommended in the adsorption processes of ionic-imprinting polyamine, ³⁴ and also for the adsorption of Pb(II) ions in an aqueous medium. ³⁵

The aim of this study was to transform blast furnace slag into a silica gel and prove its effectiveness as an adsorbent in cadmium-containing wastewater. This work was implemented in several stages. To begin, we collected, treated, and modified the blast furnace slag in order to increase its specific surface area and thus improve its adsorption power. The treatment and modification of the slag were carried out according to appropriate experimental procedures. The solid's physicochemical characterization was carried out by X-ray fluorescence (XRF) and X-ray diffraction (XRD), and its specific surface area was defined by the BET model. Subsequently, we began the process of removing cadmium from silica gel by taking into consideration the determining factors, such as contact time (tc), silica gel mass (ms), solution stirring speed (V_{ag}), pH of solution, solution temperature (T), silica gel particle size (Øs), and initial concentration of the pollutant solution. Thirdly, we investigated the interactions reacting between

the silica gel and the cadmium ions (C₀), defined the nature of the adsorption, and identified the kinetics of pollutant elimination on modified slag. The Adsorbate-adsorbent interactions were detected following the involvement of appropriate adsorption isothermal models, such as Freundlich, Langmuir, and Temkin. The nature of the process was determined following the identification of the thermodynamic parameters, i.e., free enthalpy, enthalpy, entropy, and activation energy. The adsorption kinetics were explained following the use of appropriate models, namely the pseudo-order and diffusion models. In the last phase, we undertook the desorption process. The reuse process was accomplished by treating the saturated silica gel with distilled water and different eluents, namely hydrochloric acid, phosphoric acid and nitric acid. It is important to emphasize that the raw slag samples were collected, processed, and characterized using appropriate techniques. In addition, the influencing factors were maximized by following a rigorous and precise operating protocol (experimental plan) for optimal adsorption.

2. Experimental

2. 1. Materials and Methods

The cadmium ions were assayed by atomic absorption spectrometry (Perkin Elmer 3110). The characterization of the solid samples was carried out by X-ray fluorescence (Siemens SRS 3000) and X-ray diffraction (Rigaku Ultim IV). The pH of the solution was measured by a pH meter (Ericsson). Heating of the adsorbent was carried out by a muffle furnace (Nabertherm HT16/17). Stirring was carried out using a mechanical stirrer operating at different speeds. The reagents used, namely hydrochloric acid (HCl), nitric acid (HNO3), sulfuric acid (H2SO4), and sodium hydroxide (NaOH) were of analytical grade (Merck).

2. 2. Treatment of Solid

The treatment of the blast furnace slag samples was carried out in accordance with a well-defined experimental protocol.² The modification of the slag into silica gel (SG) was carried out according to the following experimental approach:

- 50 g of treated slag were introduced into a beaker with a volume of 1 L containing NaOH (1 M).
- The mixture was stirred for 90 minutes at a partially low speed (100 rpm).
- The mixture was heated at 800 °C for 2 hours, then 20 ml of Na₂HPO₄ (10 mg/L) was added.
- The mixture obtained was further stirred (200 rpm) until homogenized;
- The treated solid was recovered by filtration, after standing for almost 8 h;
- The impurities (Al(OH)₃, Ca(OH)₂) were removed by filtration after the resting and cooling of the solution.

- The recovered filtrate was evaporated to dryness to provide sodium metasilicate Na₂SiO₃ as residue.
- The resulting sodium metasilicate (20 g) was dispersed in distilled water with gentle stirring (100 rpm) for 30 minutes.
- After this time, drops of H₂SO₄ (1M, 30 ml) were added to the stirred solution to obtain silica gel.
- Sodium sulfate (Na₂SO₄) was removed by the gradual addition of deionized water.
- The washed gel was steamed at 105°C for 8 hours and then heated in a muffle furnace at 600°C for 120 minutes.
- At the end, it was cooled, crushed, and stored in boxes.

2. 3. Specific Surface Area Determination

The specific surface area of the treated blast furnace slag and silica gel samples were determined from the amount of nitrogen adsorbed as a function of its pressure. This process was carried out at the boiling temperature of liquid nitrogen (–196 °C) and under normal atmospheric pressure (760 mmHg). 36 The experimental data of N_2 gas desorption at 77 K were evaluated with the BET model. 37

2. 4. Adsorption Process

Batch mode tests were carried out to study the adsorption of cadmium on silica gel in solution. The experimental approach consisted of adding a certain mass of silica gel to a solution containing cadmium. The solutions examined were prepared from cadmium salt in beakers of 1 L volume. The experimental conditions applied are given below:

- Contact time (tc) effects, and equilibrium estimation: $t_c = 0-180 \text{ min}$; $C_0 = 30 \text{ mg/L}$; $V_{ag.} = 200 \text{ rpm}$; pH = 4.4; T = 20 °C; $Øs = 500 \text{ }\mu\text{m}$; $m_s = 1 \text{ g}$.
- Optimization of adsorbent mass (ms): t_c = 60 min; C_0 = 30 mg/L; $V_{ag.}$ = 200 rpm; pH = 5.4; T = 20 °C; Øs = 500 μ m; m_s = 0.4, 0.6, 0.8, 1, 1.2, 1.4 g.
- Optimization of agitation speed (V_{ag}): t_c = 60 min; C_0 = 30mg/L; $V_{ag.}$ = 100, 200, 300, 400 and 500 rpm; pH = 5.4; T = 20°C; Øs = 500 µm; m_s = 1g
- Optimization of pH: t_c = 60 min; C_0 = 30 mg/L; $V_{ag.}$ = 300 rpm; pH = 2.5, 4.4, 4.7, 5.3, 6, 6.3 and 6.6; T = 25°C; Øs = 400 μ m; m_s = 1g.
- Optimization of particle size (Øs): t_c = 60 min; C_0 = 30 mg/L; $V_{ag.}$ = 300 rpm; pH = 5.8; T = 20 °C; Øs = 100, 200, 300, 400 and 500 μ m; m_s = 1g
- Optimization of Temperature (T): $t_c = 60 \text{ min}$; $C_{0.} = 30 \text{ mg/L}$; $V_{ag} = 300 \text{ rpm}$; pH = 6; T = 20, 35, 45 and 55 °C; $\emptyset = 200 \text{ } \mu\text{m}$; $m_s = 1 \text{ g}$.
- Optimization of the initial concentration (C_0), and evaluation of the maximum adsorbed quantity (qe): t_c = 60 min; C_0 = 30–300 mg/L; V_{ag} = 300 rpm; pH = 5.8; Øs = 200 μ m, T = 20 °C; m_s = 1 g.
- Study of adsorption isotherms: $t_c = 60$ min; $C_{0.} = 30$ 300 mg/L; $V_{ag} = 300$ rpm; pH = 6; Øs = 200 µm, T = 20 °C; $m_s = 1$ g.

• Study of adsorption kinetics: $t_c = 60 \text{ min}$; $C_{0.} = 30, 60,$ and 90 mg/L; $V_{ag} = 300 \text{ rpm}$; pH = 6; Øs = 200 µm, T = 20, 35, 45, 55 °C; $m_s = 1 \text{ g}$.

The adsorbed quantity of cadmium, denoted by qe and expressed in mg/g, and the adsorption yield, symbolized by R and expressed as a percentage, are obtained from equations 1 and 2.

$$q_e = \frac{c_{0} - c_t}{m_s} \times V \tag{1}$$

$$R = \frac{C_0 - C_e}{C_0} \times 100 \tag{2}$$

Where: C_0 : initial solution concentration (mg/L), C_t : solution concentration after a time t (mg/L); C_e : Concentration at equilibrium (mg/L), V: volume of the solution (L) and m_s : adsorbent mass (g).

2. 5. Point of Zero Charge (pH_{pzc})

The zero point of charge (ZPC) is a very important parameter for the evaluation of the surface charge. Indeed, this quantity allows us to decide whether the surface charge is zero (pH = pH_{pzc}), positive (pH < pH_{pzc}) or negative (pH > pH_{pzc}).² The ZPC study involved the addition of 0.1 g of silica gel (SG) samples to a solution containing KNO₃ (0.1 M). This experiment was applied at different pH, namely 2, 4, 6, 8, 10, and 12. The pH adjustment was carried out by the addition of a few drops of H₂SO₄. These solutions were shaken under operating conditions of 25°C and 200 rpm for 24 h. The ZPC was obtained at the intersection of the Δ pH (pH_f- pH_i) versus initial pH (pHi) plot with the X axis.⁷

2. 6. Desorption Process

The process recommended by Chouchane et al.¹⁸ was applied to desorb cadmium ions from silica gel. The experimental approach below was used to carry out this work:

- Using filter paper, 10 g of saturated adsorbent were obtained.
- The recovered silica gel was dehydrated for 24 hours at 105 °C.
- Utilizing H₂O and a number of eluents, including HCl, H₂SO₄, and HNO₃ at 0.05 M concentration, the cadmium desorption study was investigated.
- The desorption process was completed after 150 minutes of agitation (150 rpm).

3. Results and Discussion

3. 1. Characterization of Adsorbent

In this work, the solid samples of blast furnace slag and silica gel were studied by XRF and XRD. The mass percentages of the materials examined are shown in Table 1, while the XRD characterization is illustrated in Figures 1a and 1b. The new tests carried out by XRF of the blast furnace slag confirmed the results presented a recent research.¹⁷ Indeed, the slag examined was made up of lime (CaO: 35,2), silica (SiO₂: 40,85), alumina (Al₂O₃: 11,38), magnesium oxide (MgO: 5,03) and a fine quantity of metal

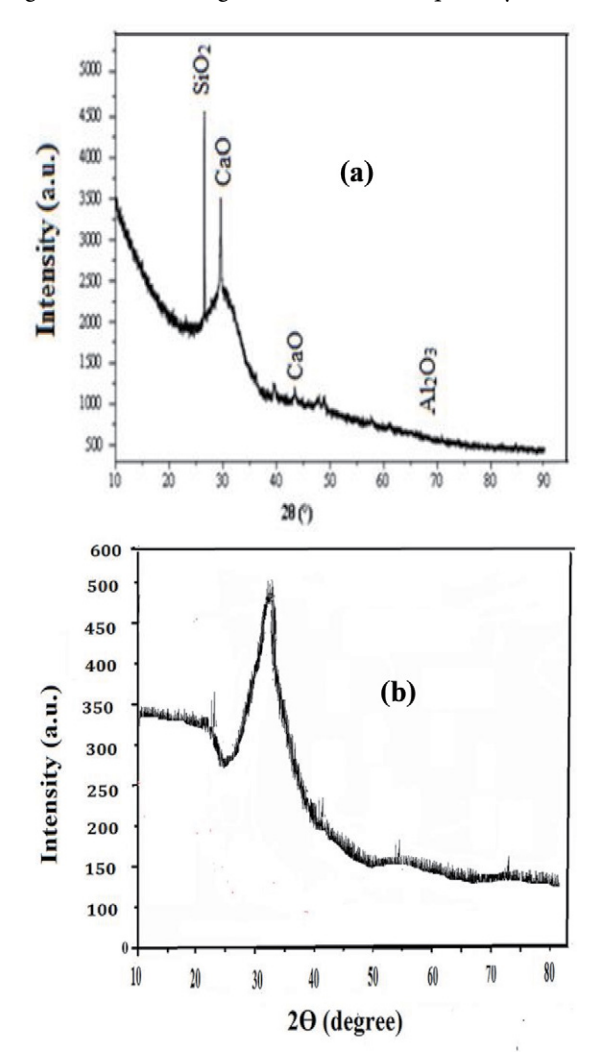


Figure 1. Diffractogram: (a) slag [19], (b) silica gel

Table 1. Chemical composition of treated blast furnace slag(BFS) [16], and silica gel (SG)

Element	Treated slag (BFS)	Silica gel (SG)				
	Mass %					
CaO	35.21	0.67				
Al_2O_3	11.38	0.46				
SiO_2	40.85	96.14				
Fe_2O_3	1.36	0				
MgO	5.03	0				
MnO	1.04	0				
K ₂ O	0.2	0				
Na ₂ O	0.99	0.61				
P_2O_5	0	0.35				
LOI	3.94	1.77				

oxide (Table 1). According to Table 1, silica gel consists of 96.14 % of silica (SiO₂).

In Figure 1a, it was determined that the results of the XRF analysis were consistent with those of the XRD analysis. High levels of lime, silica, and lower levels of alumina and magnesium oxide were detect. XRD analysis of silica gel obtained from converted blast furnace slag showed a significant increase in silica content and the absence of lime, alumina, sodium oxide and phosphorus pentoxide (Figure 2b), which have certainly dispersed in the structure.

3. 2. Contact Time Effect

The effect of contact time in adsorption processes is a crucial factor since it tells us about the equilibrium time and therefore allows us to reduce the number of tests. The impact of contact time is shown in Figure 2(a).

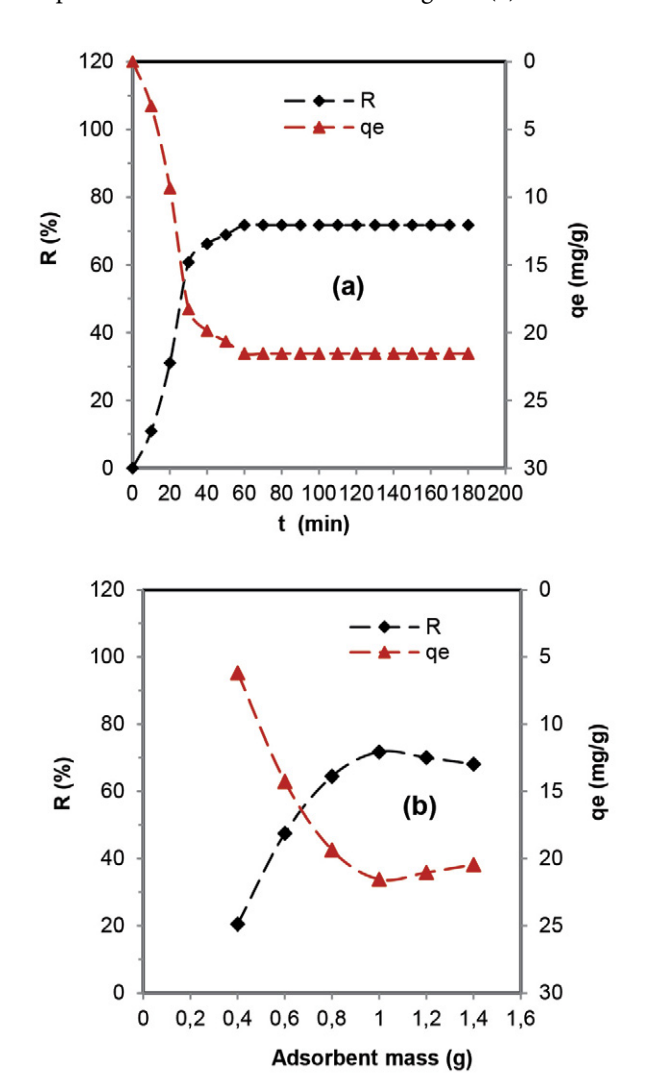


Figure 2. (a) Effect of contact time: $C_0=30$ mg/L; $V_{ag.}=200$ rpm; pH = 4.4; T = 20 °C; Øs = 500 µm; $m_s=1$ g, (b) Effect of adsorbent dosage: $t_c=60$ min; $C_0=30$ mg/L; $V_{ag.}=200$ rpm; pH = 5.4; T = 20 °C; Øs = 500 µm

According to the experimental tests, it was noticed that the saturation time of the adsorbent surface was achieved after 60 min. From Figure 2(a), we observed that this process went through three stages, namely fast, moderately slow, and stable. Between 0 and 30 min (rapid stage), the adsorption rate was 84.72%, and the adsorbed quantity increased from 0 to 18.25 mg/g. This outcome was certainly generated by the availability of multiple active adsorption sites.¹⁷ From 30 and 60 min (medium slow stage), the adsorption rate was 15.27%, and the adsorption capacity increased by 3.29 mg/g. This effect was probably due to the gradual decrease in free sites on the surface of the adsorbent.¹⁹ On the other hand, in the last stage, the adsorption rate and the sorption capacity remained constant despite the contact time increasing from 60 to 180 min. This result is undoubtedly caused by the absence of free adsorption sites, that is to say saturation of the adsorbent surface.²

According to the data in the bibliography, we observed that as cadmium adsorption of on silica gel prepared from blast furnace slag is moderately rapid. Indeed, the adsorption of cadmium on different adsorbents, such as natural Bolivian zeolite,³⁸ cellulose-embedded polyacrylonitrile/amidoxime,³⁹ biochar derived from a manure mix,⁴⁰ Mn oxide-modified pine biochar,⁴¹ and Fe₃O₄ nanoparticles loaded sawdust carbon,⁴² was accomplished after 60, 90, 120, 60, 30 and 90 min, respectively.

3. 3. Effect of Adsorbent Dosage

The effect of adsorbent mass on cadmium adsorption on silica gel prepared from blast furnace slag was examined using different masses, namely 0.4, 0.6, 0.8, 1, 1.2, and 1.4 g (Figure 2(b)).

According to the experimental tests, two stages were observed: one strongly increasing from 0.4 to 1g and the other slightly decreasing from 1 to 1.4g. At first, we observed that the adsorption rate and capacity increased by 52.26 % and 15.38 mg/g, respectively. While for the second stage, they had decreased by 3.66% and 1.1 mg/g, respectively. The increase in the adsorption rate and capacity were surely generated by the existence of many unoccupied adsorption sites. All The reduction in adsorption efficiency is undoubtedly generated by the constant number of cadmium ions in solution in relation to the number of active sites in continuous growth. For this purpose we opted for 1g as the optimal mass of silica gel in this process.

3. 4. Effect of Agitation Speed

In these processes, medium agitation is a significant step since it contributes considerably to the pollutant transport from the liquid to the solid phase. ¹⁷ For this purpose, we introduced this adsorption process. The stirring speeds (V_{ag}) exploited are 100, 200, 300, 400, and 500 rpm (Figure 3(a)).

According to the experimental test results, we discovered that the adsorption of cadmium was more efficient at 300 rpm. Indeed, it was observed that the adsorption yield and capacity systematically progressed between 100 and 300 rpm (Figure 3a). In this speed range, the values of adsorption efficiency and capacity increased from 59.46% to 78.26% and from 17.84 mg/g to 23.48 mg/g, respectively. The cadmium adsorption was certainly generated by an increase in the diffusion coefficient and, consequently, a better diffusion of cadmium ions from the solution to the adsorbent surface of the silica gel. 47,48

From the same source (Figure 3(a)), we observed that between 300 and 500 rpm, the adsorption rate and capacity remained constant (78.26 %, 23.48 mg/g). This result was certainly caused by the cessation of external diffusion and, consequently, the elimination of the liquid barrier to mass diffusion. 19 Based on this information, we opted for a V_{ag} stirring speed of 300 rpm as the most suitable.

3. 5. Effect of Initial pH

It is widely recognized that solution ph has a significant influence on the adsorption process, particularly with respect to the adsorption of metal pollutants, due to its impact on adsorbent surface charge and speciation. metallic pollutants in aqueous environments. ^{2,19} In order to better understand the experimental results from this stage, it is essential to identify the zero charge point (ZPC). The identification of the point of zero charge (ZPC or pHzpc) is demonstrated in Figure 3(b). The study of the influence of pH is shown in Figure 3(c).

From the analysis of Figure 3(c), we determined that the value of zero charge point (pH $_{\rm ZPC}$) is 4.2. This outcome allowed us to predict that the adsorption of cadmium ions is more efficient at pH > 4.2. It is true that the cadmium removal efficiency greatly improved when the pH exceeded the pH $_{\rm ZPC}$, resulting in an increase of 58.76% and 17.63%, respectively, in the yield and the amount removed between pH 4 ,2 and 6 (Figure 3(c)). It is important to mention that the increase in the rate of cadmium elimination at pH > 6 was also generated by chemical precipitation. Indeed, it has been cited in the literature that the formation of Cd(OH) $_2$ starts progressively at pH > 6.49-52 From these details, we concluded that the adsorption of cadmium on silica gel took place efficiently at pH 6 under the effect of electrostatic interactions.53,54

Regarding a pH varying from 2.5 to 4, we observed that the adsorption rates and the experimental adsorbed quantity were low. The adsorption inefficiency was mainly caused by the electrostatic repulsion effect instituted between the adsorbent and the adsorbate.²⁰ In addition, the excess H⁺ constituted a partial obstacle between cadmium ions and the adsorbent surface.¹⁷ The interaction between the adsorbent surface of silica and cadmium in solution is shown in Figure 4

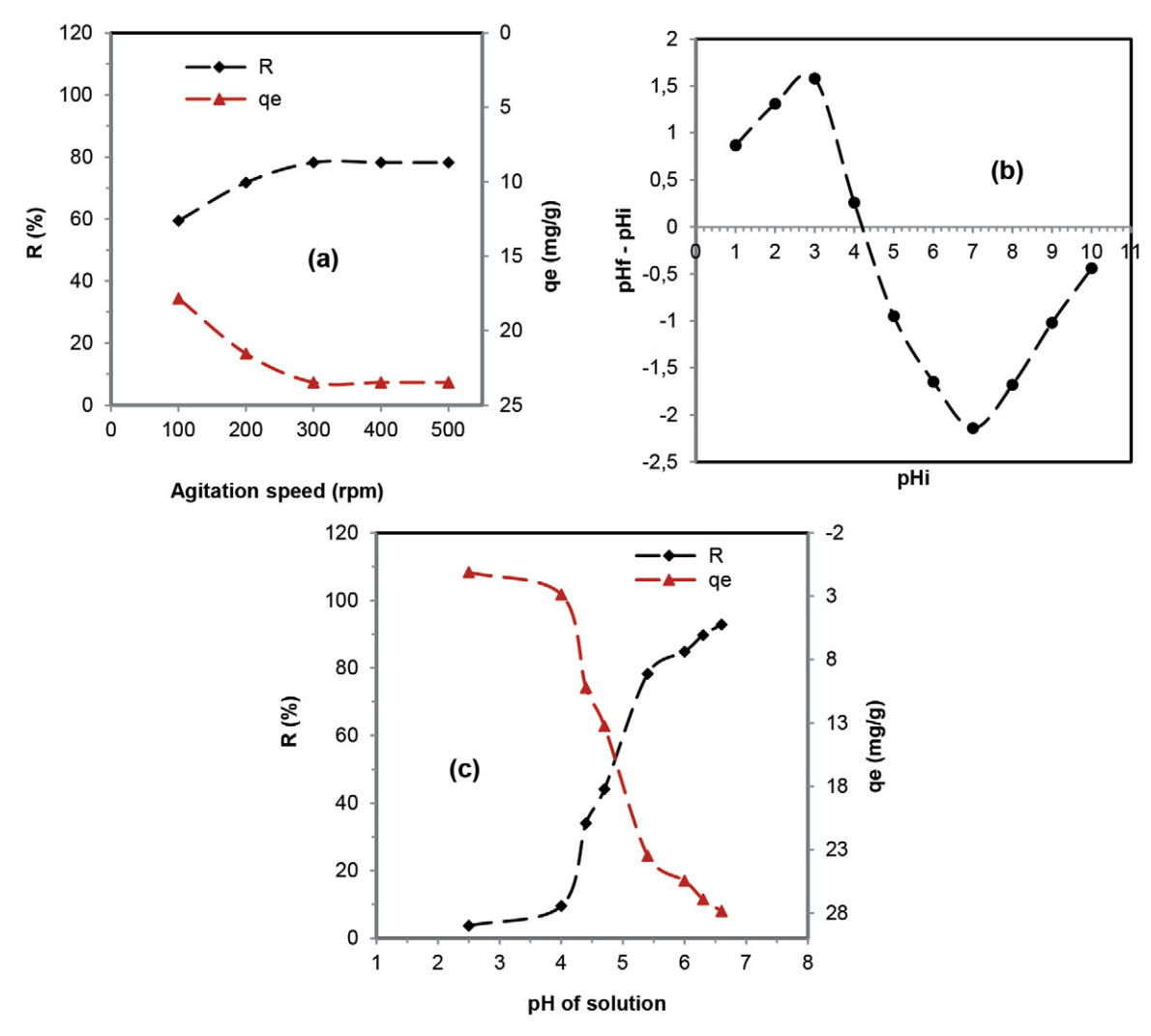


Figure 3. (a) Effect of agitation speed: $t_c = 60$ min; $C_0 = 30$ mg/L; pH = 5.4; T = 20°C; Øs = 500 μ m; m = 1g, (b) Zeta potential as a function of solution pH, (c) Effect of initial pH: $t_c = 60$ min; $C_0 = 30$ mg/L; $V_{ag.} = 300$ rpm; pH = 2.5, 4.4, 4.7, 5.3, 6, 6.3 and 6.6; T = 25°C; Øs = 400 μ m; m = 1g

According to the study by M'barek et al.,⁸ the ideal pH for the adsorption of cadmium on mesoporous silica, zeolite-supported zerovalent iron nanoparticles and cellulose was 6. In the same order of ideas, it has also been evoked that cadmium was efficiently adsorbed on natural Bolivian zeolite treated with NaCl,³⁸ on polyacrylonitrile/amidoxime covered with cellulose, ³⁹ on wastewater treatment sludge,⁴⁰ and on kaolin,43 with a pH ranging from 5 to 6.

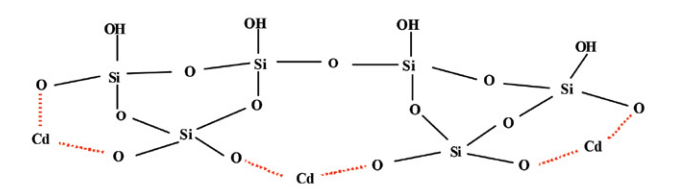


Figure 4. Diagram of the cadmium adsorption mechanism on the silica gel: Presentation of the electrostatic interaction between O^- and Cd^{++}

2. 6. Effect of Particle Size

The influence of solid particle size (\emptyset s) on the sorption process of cadmium in solution by silica gel was discussed for different sizes, namely 100, 200, 300, 400, and 500 μ m (Figure 5(a)).

The experimental results indicated that cadmium adsorbed efficiently at a particle size (Øs) of 200 μ m. It was observed that by reducing the particle size from 500 to 200 μ m, the experimental adsorption capacity and yield evolved by 17.73% and 5.32 mg/g, respectively (Figure 5(a)). It is highly plausible that the main reason for this efficiency lies in the reduction in the particle size of the solid, which resulted in an extension of the adsorption surface. ^{16,55} Indeed, the larger the surface area, the more efficient the adsorption since this phenomenon is controlled by the ratio between the surface area of the adsorbent and the volume of the adsorbate. ⁵⁶ It should be emphasized that for a particle size (Øs) of 100 μ m, we observed a divergence from what was mentioned previously. Between 200 and 100 μ m,

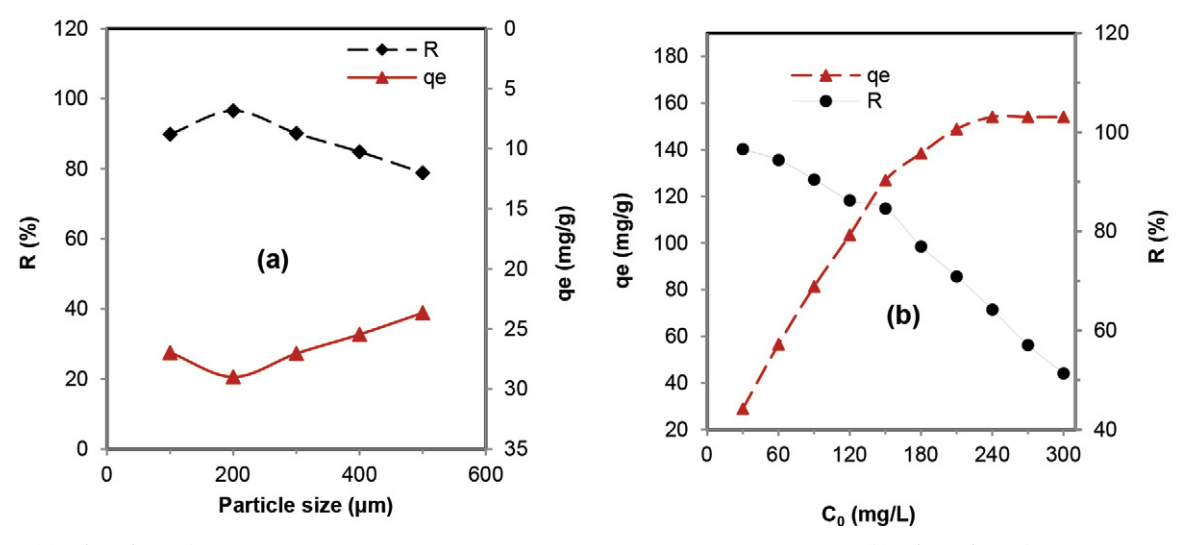


Figure 5. (a) Effect of particle size: t_c = 60 min; C_0 = 30 mg/L; $V_{ag.}$ = 300 rpm; pH = 5.8 ;T = 20 °C; ms = 1g, (b) Effects of Initial Concentration: t_c = 60 min; V_{ag} = 300 rpm; pH = 5.8; Øs = 200 μ m, T = 20 °C; ms = 1 g

the adsorption capacity and yield decreased by 6.73% and 2.02 mg/g, respectively. The regression in the efficiency of adsorption can certainly be due to the agglomeration of the silica gel particles, that is to say, to their evolution into larger particles (coalescence phenomenon).^{17,57}

3. 7. Effects of Initial Concentration

In this process, the study of the influence of the initial concentration is decisive since it allows us to trace the experimental adsorption isotherms and thus allows us to determine the maximum adsorption quantity. In order to achieve this objective, we examined the action of the initial concentration of 30 to 300 mg/L under specific operating conditions (Figure 5(b)).

From the experiments carried out, we observed that the value of the adsorption capacity progressed with the rise in the initial concentration, and then it became constant despite the supply of cadmium ions (Figure 5(b)). The adsorption capacity increased from 28.98 to 154.11 mg/g for an initial concentration of $30 \le C_0 \le 240$ mg/L. It is likely that this performance is attributable to the continued increase in the initial concentration, which generated a strong driving force. The latter made the transfer of cadmium ions from the solution to the adsorbent easier by reducing the resistance to mass transfer. ^{17,58,59} On the other hand, from $C_0 \ge$ 240 mg/L, the adsorption capacity remained constant (154.11 mg/g). The stability of the adsorption capacity was certainly due to the saturation of the adsorbent surface and also to the elimination of external diffusion resistances. 16,19 The experiment results also showed that the cadmium adsorption rate decreased with increasing initial concentrations (Figure 5(b)), where its value gradually dropped from 96.6 to 51.37%. The progressive decrease in the adsorption rate was probably generated by the uninterrupted addition of cadmium ions by supply to an invariable active surface (constant number of active adsorption sites).^{2,18}

By examining the maximum amount of cadmium adsorbed by different adsorbents, including silica-coated metal organic framework (634 mg/g),⁵ mesoporous silica (3.62 mg/g),⁸ zerovalent iron supported by a zeolite (63.14 mg/g),⁸ orange peels (59.5 mg/g),⁸ cellulose chelating sulfur (54.7 mg/g),⁸ bone meal apatite (116.16 mg/g),¹⁴ eggshell (217.4 mg/g),¹⁵ and NaCl-treated Bolivian natural zeolite (25.6 mg/g),³⁸ it has been established that silica gel prepared from blast furnace slag has a capacity fairly high adsorption rate (154.11 mg/g) and constitutes a promising adsorbent for the removal of cadmium in wastewater.

3. 8. Adsorption Isotherms

Adsorption isotherm models were approached to evaluate the maximum quantities adsorbed and also to specify the interactions reacting in this process. With this in mind, we selected for suitable models, namely the Freundlich, Langmuir and Temkin models. ^{17,51} Their linear forms are represented by equations 3, 5, and 6, respectively. Equation 4 describes the separation factor $R_{\rm L}$ of the Langmuir model.

$$log q_e = log k_F + \frac{1}{n} log C_e \tag{3}$$

$$\frac{c_e}{q_e} = \frac{1}{q_{max}} C_e + \frac{1}{q_{max}k_L} \tag{4}$$

$$R_L = \frac{1}{1 + C_0 b} \tag{5}$$

$$qe = B_T ln A_T + B_T ln Ce (6)$$

Where q_{max} , qe: adsorbed capacity maximum and at equilibrium (mg/g), Ce, C_0 : concentration at equilibrium and initial (mg/L), k_L : Langmuir constant (L.mg⁻¹), k_F : Freundlich constant (mg.g⁻¹) (ml.mg⁻¹)^{1/n}, 1/n: adsorption Intensity, $B_T = \frac{RT}{b_T}$, A_T : equilibrium binding constant (L/g), R: universal gas constant (8.314 J/mol/K), T: absolute temperature in Kelvin, b_T : constant related to heat of sorption (kJ kmol⁻¹).

Table 2. Isotherm parameters for cadmium adsorption

Freundlich				Langmuir				Temkin		
k_F	1/n	R^2	q_{max}	k_L	R^2	R_L	\boldsymbol{b}_T	A_T	R^2	
$(mg.g^{-1})(ml.mg^{-1})^{1/}$			(mg/g)	(L.mg ⁻¹)			(kJ/mol)	(L/g)		
27.81	0.34	0.94	153.84	0.154	0.99	0.021- 0.17	0.92	2.26	0.95	

The plots of the Freundlich, Langmuir Temkin models and their adsorption isotherms are reproduced in Figures 6(a), 6(b), 6(c), and 6(d). The parameter values of the models discussed are displayed in Table 4.

From the results obtained (Table 2), it was proven that the Langmuir model is the best fitted to the experimental points. Indeed, the correlation coefficient of the Langmuir model ($R^2 = 0.99$) was higher than those of Freundlich ($R^2 = 0.94$) and Temkin ($R^2 = 0.95$). In addition, the value of the theoretical adsorption capacity resulting from the Langmuir model (154.11 mg/g) was closer to the experimental adsorbed capacity (153.84 mg/g). From Figure 6(d), we observed that the shape of the plot of the Langmuir isotherm had the same shape as the shape of the

experimental isotherm (type 1). They increase gradually before stabilizing by establishing a saturation level. This outcome confirmed to us that the cadmium adsorption on the silica gel was accomplished on a monolayer and homogeneous surface. 22,31,60 The value of 1/n corresponded to 0.34 (Table 2) and the value of $R_{\rm L}$ was between 0 and 1, thus affirming the favorability of the adsorption process. 18,23 The value of the Temkin model parameter (b_T) indicated that the adsorption is physical (b_T < 8 Kj/mol). 60

3. 9. Kinetics of Adsorption

Reputed models in the field of solid-liquid adsorption, namely, pseudo-first-order (PFO), pseudo-sec-

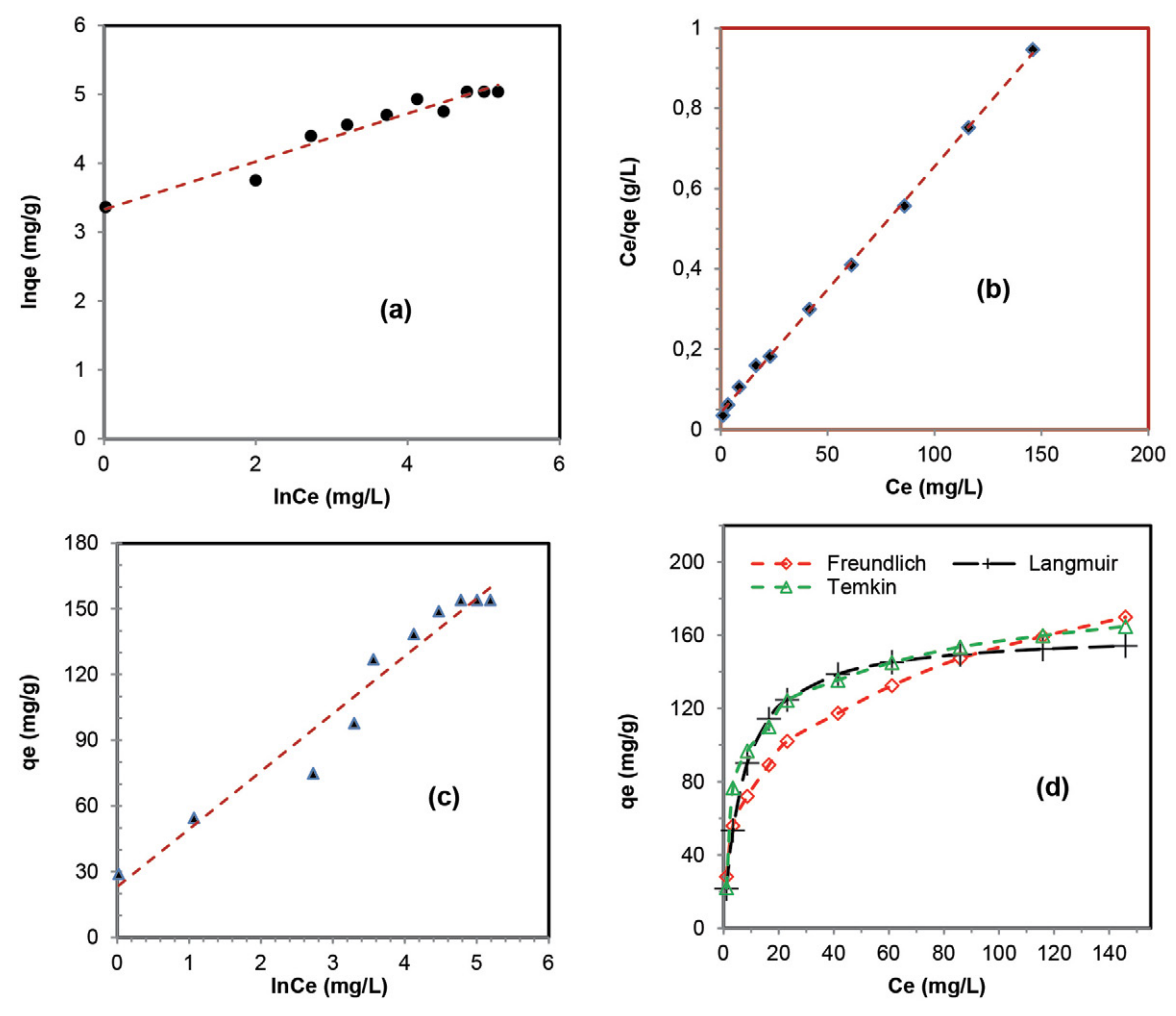


Figure 6. (a) Freundlich model presentation, (b) Langmuir model presentation, (c) Temkin model presentation, (d) Presentations of adsorption isotherms. $t_c = 60 \text{ min}$; $C_{0.} = 30-300 \text{ mg/L}$; $V_{ag} = 300 \text{ rpm}$; pH = 6; Os = $200 \text{ }\mu\text{m}$, $T = 20 \text{ }^{\circ}\text{C}$; m = 1 g

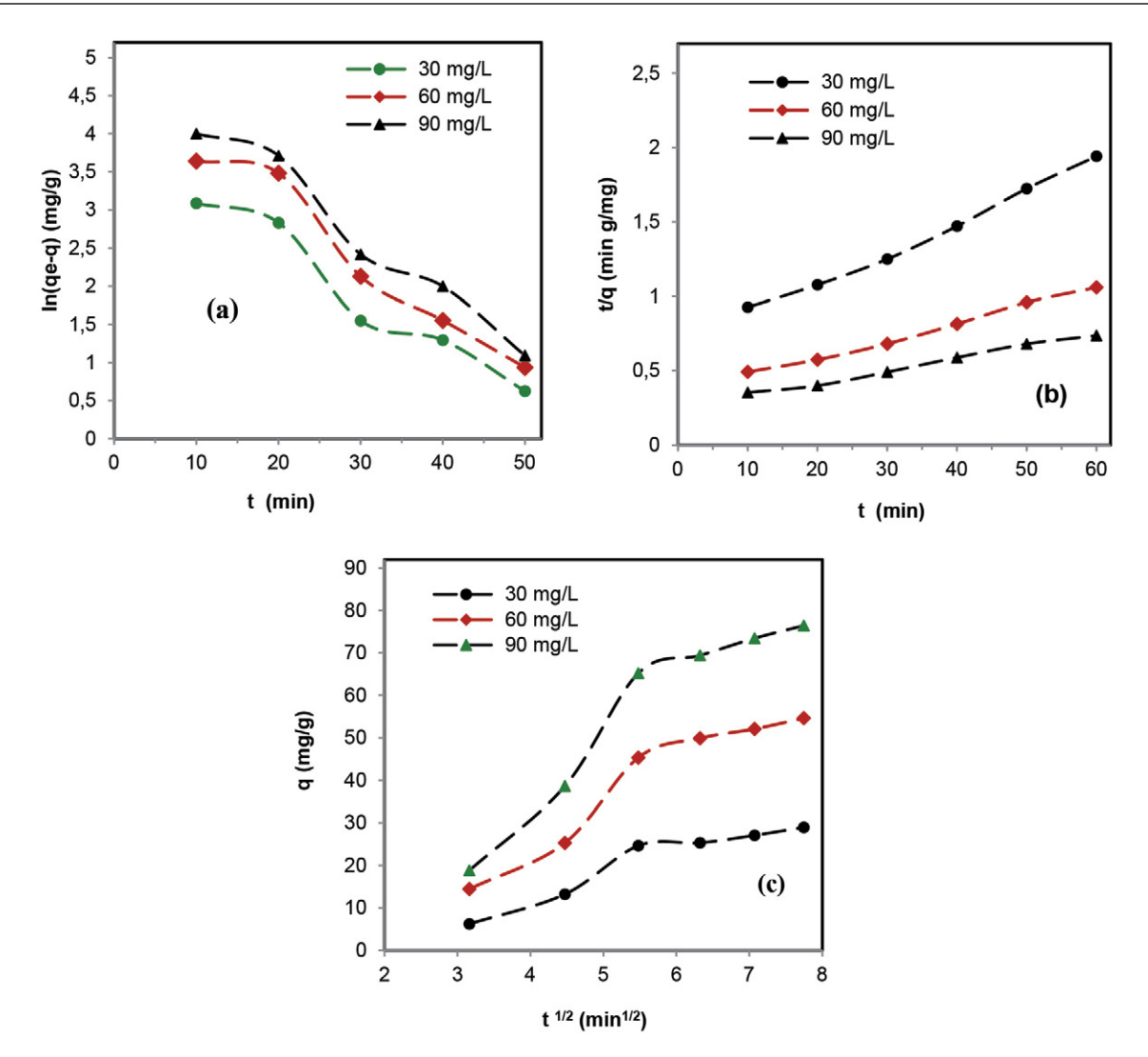


Figure 7. (a) pseudo-first-order model, (b) pseudo-second-order model, (c) internal diffusion: $t_c = 60 \text{ min}$; $C_{0.} = 30-300 \text{ mg/L}$; $V_{ag} = 300 \text{ rpm}$; pH = 6; $\varnothing s = 200 \text{ } \mu m$, $T = 20 \text{ }^{\circ} C$; m = 1 g

ond-order (PSO), and intraparticle diffusion (IPD) kinetic models, have been used to discuss the kinetics of adsorption of cadmium in solution on silica gel (SG) prepared from slag. The PFO, PSO and IPD models are described by equations 7,8, and 9 respectively.^{18,35}

$$\ln(q_e - q) = -k_L t + \ln q_e \tag{7}$$

$$\frac{t}{q} = \frac{1}{k_B q_e^2} + \frac{t}{q_e} \tag{8}$$

Table 3. Kinetic parameters

$$q = k_W \sqrt{t} + C_{In} \tag{9}$$

where q and qe: quantity adsorbed at time t and at equilibrium (mg/g), t: time of adsorption process, k_L : pseudo-first-order constant (min $^{-1}$), k_B : pseudo second order constant (g/mg min), k_W : internal diffusion constant (mg/m. min $^{1/2}$), and $C_{\rm In}$: intercept.

Plots of $\ln(\text{qe-q})$ versus t, t/q versus t, and q versus \sqrt{t} are illustrated in Figures 7(a), 7(b), and 7(c), respectively. The adjustment results are produced in Table 3.

C_0	qe_{exp}	Pseudo-first-order			Pseudo-second-order			Intraparticle diffusion		
(mg/L)	(mg/g)	K_L (min ⁻¹)	qe_{theo} (mg/g)	R^2	K_B (g/mg min)	qe_{theo} (mg/g)	R^2	C_{int}	K_W (mg/g.min	R^2
30	28.98	0.065	45.40	0.94	0.086	29.41	0.99	8.1	5.09	0.91
60	56.64	0.072	90.91	0.95	0.008	58.82	0.99	5.09	9.29	0.92
90	81.43	0.077	134.83	0.94	0.006	83.33	0.99	0.91	12.97	0.91

According to Table 3, it appears that the regression coefficients of PSO ($R^2 \geq 0.99$) are higher than those of PFO ($R^2 \leq 0.95$). Furthermore, the estimated adsorption capacities of PSO were practically equivalent to the actual capacities. From this information, we judged that the adsorption process of cadmium on SG follows pseudo-second order kinetics. 16,35

It is reported in the literature that cadmium adsorbed on various adsorbents, such as silica-coated metal organic framework, Canna indica-derived biochar, thermally activated sepiolite, layered double hydroxide nanoparticles stabilized on iron slag, modified biochar, virgin and acid-modified kaolinite clay, and calcium carbonate from eggshells, exhibits pseudo-second-order kinetics. 5,6,9,12-15

From Figure 7(c), it was observed that the plots were multilinear and did not converge towards the origin, which is not in agreement with the conditions formulated by Weber and Morris (linearity of straight lines and their passage through the origin).⁶¹ Furthermore, it was specified that the correlation coefficients were greater than 0.9 (Table 3). The mentioned data allowed us to conclude that intraparticle diffusion is not the only mechanism regulating the adsorption of cadmium on silica gel.^{17,62,63} Indeed, the adsorption of cadmium was first controlled by external diffusion due to agitation of the solution, ⁴⁷ then by intraparticle diffusion.

3. 10. Effect of Temperature

In this passage, we discussed the effect of temperature on the adsorption of cadmium by silica gel, taking into consideration various temperature (Figure 8(a)). The experiments accomplished have unequivocally demonstrated that the adsorption efficiency of cadmium decreases when the temperature of the medium increases. In fact, a reduction of 28.73% in yield and 8.62 mg/L in adsorption capacity was recorded due to an increase in temperature. (Figure 8(a)). The lowering of cadmium adsorption efficiency with increasing solution temperature was certainly caused by the evolution of the random movement of cadmium ions, attenuating the interdependence between adsorbent and adsorbate.⁶⁴ Taking these results into account, we predicted that cadmium removal by adsorption on silica gel is exothermic.^{21,65,66}

It should be noted that, contrary to what has been observed, temperature can cause an increase in cadmium

adsorption, as reported in the literature. Significant improvements in the adsorption of cadmium in solution were found when the temperature was increased with different adsorbents, including pristine and acid-modified kaolinite clay, electrospun composite nanofibre, modified biochar, gel-like weak acid resin, acid-modified chili peppers, and NiO nanoparticles. 10,13,14,67,68,69

With the same purpose, a thermodynamic study was carried out to identify the nature and mechanisms of interaction favoring this process. The explanation of these effects (nature and mechanism of interaction) strongly depends on the values of the thermodynamic parameters, namely ΔG° , ΔH° , ΔS° and Ea. Equation 10 was used to calculate ΔG° , while equation 11 was used to determine ΔH° and ΔS° , and Ea was deduced from equation 13. 2,16,17 Equation 12 describes the distribution coefficient $k_d.^{19}$ The Arrhenius equation (Eq. 13) was used to calculate the activation energy. 2

$$\Delta G^0 = -RTlnk_d$$
 10)

$$lnk_{d} = \frac{\Delta H^{0}}{R} \times \frac{1}{T} + \frac{\Delta S^{0}}{R}$$
 (11)

$$k_d = \frac{c_i - c_e}{c_e} \times \frac{v}{M} = \frac{q_e}{c_e} \tag{12}$$

$$lnk_{app} = lnA - \frac{E_a}{RT}$$
 (13)

Where ΔG° is the Gibbs free energy (kJ/mol), ΔS° is entropy (kJ/ K), ΔH° is enthalpy (kJ/mol), R is the universal gas constant (8.314 J/mol.K), K_d is distribution coefficient (L/g), Ea is activation energy (kJ/mol), k_{app} apparent constant (g/L.min), T is the absolute temperature (K) and A is frequency factor.

The apparent constant k_{app} was calculated from the function $\ln(Ct) = f(t)$ at different temperatures (20, 35, 45, and 55 °C). Van't Hoff and Arrhenius plots are represented by Figures 8(b) and 8(c). The values of free enthalpy, enthalpy, entropy, activation energy, apparent constant and distribution coefficient are displayed in Table 4.

From Figure 8(b), it was noticed that there was a good interdependence between the Van't Hoff model and the experimental data ($R^2 = 0.99$) (Table 4).² The decrease in the distribution coefficient (K_d) with increasing temperature made it possible to clarify that the adsorption of cadmium was favorable in the least heated solutions.^{19,70}

From Table 4, it was identified that the Gibbs energy values are negative and less than 20 kJ/mol, which ex-

 $\textbf{Table 4.} \ \textbf{Thermodynamic parameters of cadmium adsorption}$

T (K)	ΔH° (kJ/mol)	ΔG° (kJ/mol)	ΔS° (kJ/K)	Ea (kJ/mol)	R^2	K_d (L/g)	k _{app} (g/L.min)
293		-18.11				1.79	5.22×10 ⁻²
	-6.98		-25.67×10^{-3}	8.45	0.99		6.32×10^{-2} 6.86×10^{-2}
							8.54×10^{-2}
308 318 328	-6.98	-18.87 -19.38 -19.74	-25.67×10 ⁻³	8.45	0.99]	1.69 1.60 1.56

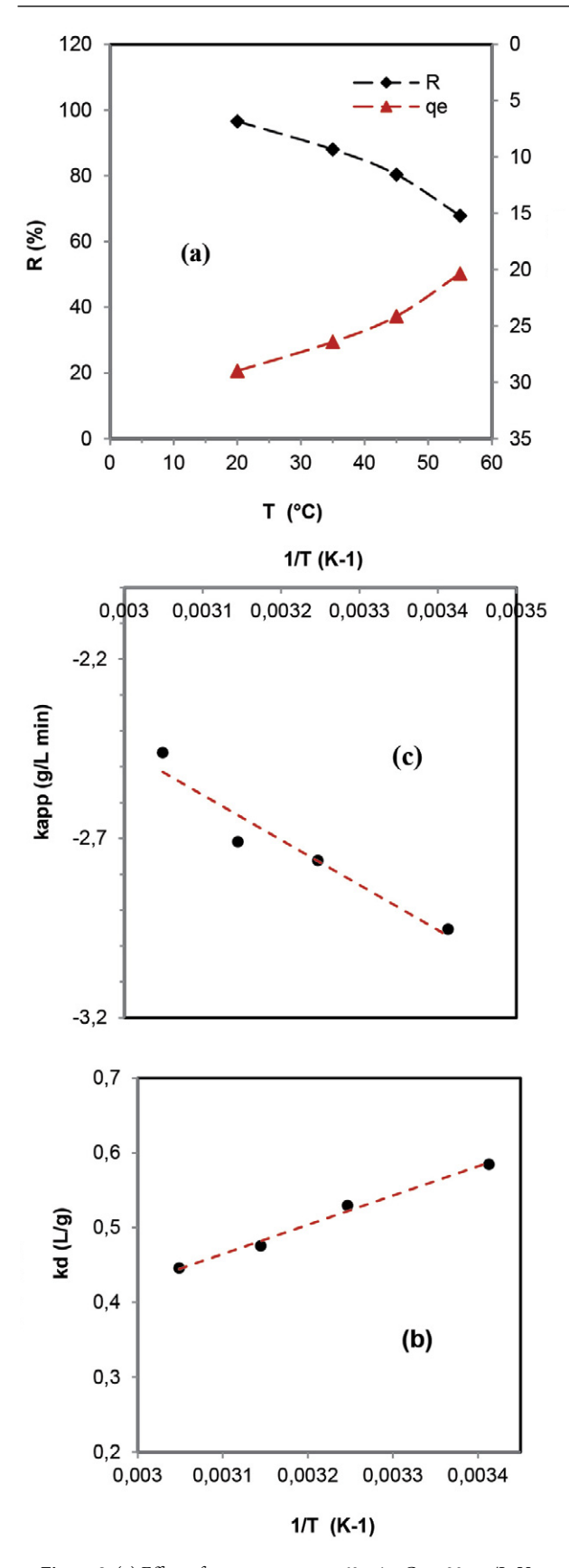


Figure 8. (a) Effect of temperature: $t_c=60$ min; $C_{0.}=30$ mg/L; $V_{ag}=300$ rpm; pH = 6; T = 20, 35, 45 and 55 °C; Ø = 200 μ m; m = 1 g, (b) Van't Hoff equation plot, (c) Arrhenius equation plot

plained that the sorption of cadmium is spontaneous and occurred under the influence of physical interactions. 17,39 The increase in the temperature of the solution resulted in a regression of ΔG° from -18.11 to -19.74 kJ/mol, thus demonstrating that mass transfer is inversely proportional to the temperature of the medium. 65,71 The negative value of the enthalpy (-6.98 kJ/mol) revealed that this process is exothermic (Table 4). 18,39 In addition, it also certified that this cadmium removal process is a physical adsorption, whose enthalpy value is less than 40 kJ/ mol. 20,72 The negative value of entropy highlighted the reduction of randomness at the adsorbent-adsorbate interface (Table 4).16,55 The reduction in random displacements at the solid-liquid interface was probably caused by the considerable electrostatic interaction between the cadmium ions and the adsorbent.73,74 Based on the activation energy value (Table 4), we reaffirmed that the removal of cadmium in solution by silica gel is physical adsorption.2,62,75

From this information, we could conclude that the adsorption of cadmium on silica gel was spontaneous, exothermic, and less entropic. Furthermore, we deduced that the elimination was carried out by physical adsorption under the effect of electrostatic interactions. It should be emphasized that the adsorption of cadmium on various adsorbents is generally a spontaneous process, as clearly demonstrated in the literature. ^{13,39,44,67,69,76}

3. 11. Reuse of Adsorbent

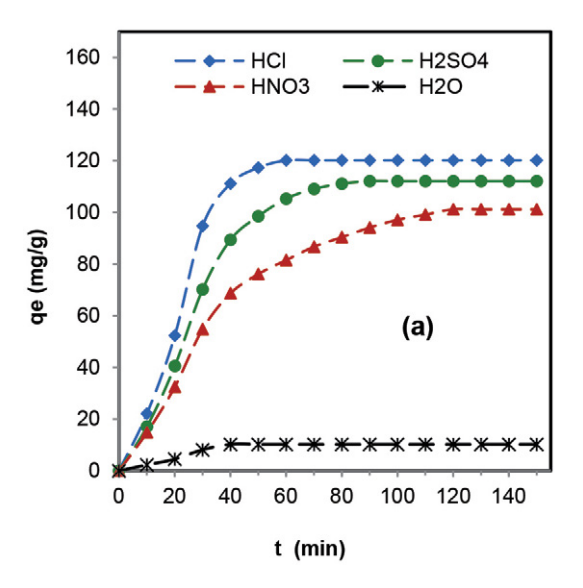
Figure 9(a) illustrates the kinetics of cadmium desorption from silica gel in the presence of different solutions. Figure 9 (b) illustrates the adsorption/desorption rate of cadmium under the effect of HCl at 0.05 M.

From the experimental data, it was noticed that the presence of HCl in solution significantly facilitated the desorption of cadmium ions from the saturated silica gel (Figure 9(a)). This outcome can be caused by the formation of a large number of H⁺ protons, which will affect the nature of the adsorbent surface.⁷⁷ According to Figure 9(b), it was specified that the silica gel has the ability to be reused for five consecutive cycles using 0.05 M hydrochloric acid as the eluent. It should be clarified that the loss of mass and the exhaustion of active adsorption sites are surely responsible for the inefficiency of the desorption process after the fifth cycle.^{20,78}

It is important to mention that the desorption percentage of cadmium ions from the adsorbent surface of saturated silica gel was examined using Equation 14.

$$Desorption \ rate = \frac{q_{des}}{q_{ads}} \times 100 \tag{14}$$

Where q_{ads} is the adsorbed quantity at equilibrium (mg/g) for cycle I and q_{ads} is the desorbed quantity at equilibrium (mg/g) of each cycle.



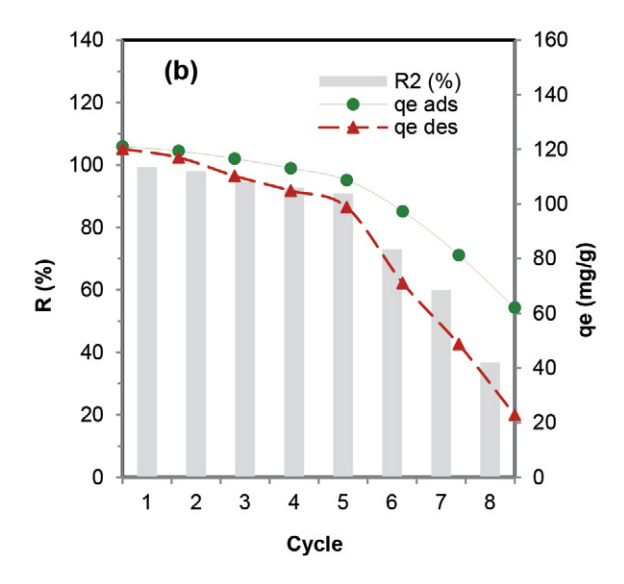


Figure 9. (a) desorption kinetics, (b) adsorption and desorption performance of cadmium

4. Conclusion

This study investigated the batch adsorption of cadmium ions onto silica gel (SG) prepared from blast furnace slag. The results demonstrated that silica gel contained 96.14% SiO₂. Its ZPC corresponds to pH 4.2, and its specific surface area is 484 m²/g. From the experimental results, it was found that the adsorption capacity of cadmium on the silica gel (qe = 154.11 mg/g) was particularly influenced by the determining parameters, namely contact time (60 min), stirring speed (300 rpm), dosage of the adsorbent (1 g/L), pH (6), temperature (20 °C), particle size (200 µm), and initial concentration (240 mg/L). Modeling of experimental data indicated that the Langmuir model $(R^2 = 0.99; q_{max} = 134.06 \text{ mg/g})$ is the most commonly adopted to represent the adsorption of cadmium on silica gel, thus affirming a monolayer adsorption on homogeneous active sites. The R_L and n values of the Langmuir and Freundlich models, respectively, revealed that the adsorption was favorable. The value of b_T from the Temkin model demonstrated that the adsorption was accomplished physically. The kinetic study showed that adsorption follows pseudo-second-order kinetics ($R^2 \ge 99$). Furthermore, it clarified that the transport of cadmium was carried out through external and intraparticle diffusion. The values of Gibbs energy ($\Delta G^{\circ} < 0 \text{ kJ/mol}$), enthalpy ($\Delta H^{\circ} < 0 \text{ kJ/mol}$) mol), and entropy (ΔS° < 0 J/K) demonstrated, respectively, that the adsorption of cadmium on silica gel is spontaneous, exothermic, and less entropic. The values of enthalpy (ΔH) and activation energy (Ea) revealed that this process was physically accomplished under the effect of electrostatic attraction. The desorption process demonstrated that the application of 0.05 M HCl as eluent significantly improved its reuse for five cycles. From this study, we reasoned that silica gel can be exploited as a reliable adsorbent to remove cadmium ions from wastewater.

Conflict of Interest

The authors declare that they have no known competing financial interests or personal relationships that could have appeared to influence the work reported in this paper. Competing interests.

5. References

- M. Mansoorianfar, H. Nabipour, F. Pahlevani, Y. Zhao, Z. Hussain, A. Hojjati-Najafabadi, H.Y. R. Hoang Pei, *Environ. Res.* 2022, 214, 114113. DOI:10.1016/j.envres.2022.114113
- T. Chouchane, A. Boukari, *Anal. Bioanal. Chem. Res.* 2022, 9, 381–399. DOI:10.22036/ABCR.2022.325691.1716
- V. K. Gupta, P. J. M. Carrott, M. M. L. Ribeiro Carrott, Suhas, Crit. Rev. Environ. Sci. Technol. 2009, 39, 783–842.
 DOI:10.1080/10643380801977610
- K. Pyrzynska, J. Environ. Chem. Eng. 2019, 7, 102795.
 DOI:10.1016/j.jece.2018.11.040
- S. Ul Mehdi, K. Aravamudan, *Mater. Today: Proc.* 2022, 61, 487–497. DOI:10.1016/j.matpr.2021.12.304
- X. Cui, S. Fang, Y. Yao, T. Li, Q. Ni, X. Yang, Z. He, Sci. Total Environ. 2016, 562, 517–525.
 DOI:10.1016/j.scitotenv.2016.03.248
- 7. F. Zhou, G. Ye, Y. Gao, H. Wang, S. Zhou, Y. Liu, C. Yan, *J.*
- Hazard. Mater. **2021**, 423, 127104. **DOI:**10.1016/j.jhazmat.2021.127104
- I. M'barek, H. Slimi, A. K. D. AlSukaibi, F. Alimi, R. Hadj Lajimi, L. Mechi, R. ben Salem, Y. Moussaoui, *Arab. J. Chem.* 2022, 15, 103679. DOI:10.1016/j.arabjc.2021.103679
- L. Semerjian, J. Hazard. Mater. 2010, 173, 236–242.
 DOI:10.1016/j.jhazmat.2009.08.074
- S. Tasharrofi, Z. Rouzitalab, D. M. Maklavany, A. Esmaeili, M. Rabieezadeh, M. Askarieh, A. Rashidi, H. Taghdisian, *Sci. Total Environ.* 2020, 736, 139570.

- DOI:10.1016/j.scitotenv.2020.139570
- M. Mousakhani, N. Sarlak, *Mater. Chem. Phys.* 2020, 256, 123578. DOI:10.1016/j.matchemphys.2020.123578
- T. S. Hussein, A. A. H., Faisal, Arab. J. Chem. 2023, 16, 105031. DOI:10.1016/j.arabjc.2023.105031
- T. Liu, Y. Lawluvy, Y. Shi, J. O. Ighalo, Y. He, Y. Zhang, P-S. Yap, *J. Environ. Chem. Eng.* 2022, 10, 106502.
 DOI:10.1016/j.jece.2021.106502
- 14. L. S. Mustapha, A.S. Yusuff, P.E. Dim, *Heliyon* **2023**, *9*, e18634. **DOI:**10.1016/j.heliyon.2023.e18634
- 15. K. Annane, W. Lemlikchi, S. Tingry, *Biomass Conv. Bioref.* **2021**, *13*, 6163–6174. **DOI:**10.1007/s13399-021-01619-2
- T. Chouchane, O. Khireddine, A. Boukari, *J Eng. Appl. Sci.* 2021, 68, 00039–3. DOI:10.1186/s44147-021-00039-3
- T. Chouchane, S. Chibani, O. Khireddine, A. Boukari, *Iran. J. Mater. Sci. Eng.* 2023, 20, 1–13. DOI:10.22068/ijmse.3011
- T. Chouchane, A. Boukari, O. Khireddine, S. Chibani, S. Chouchane, *J. Eng. Appl. Sci.* 2023, 70, 58.
 DOI:10.1186/s44147-023-00218-4
- T. Chouchane, A. Boukari, O. Khireddine, S. Chibani, S. Chouchane, *Eurasian J. Chem.* 2023, 38, 115–130.
 DOI:10.31489/2959-0663/2-23-3
- T. Chouchane, O. Khireddine, S. Chibani, A. Boukari, *Anal. Bioanal. Chem. Res.* 2023, 10, 251–268.
 DOI:10.22036/ABCR.2022.365182.1843
- C. Li, X. Li, Y. Yu, Q. Zhang, L. Li, H. Zhong, S. Wang, J. Ind. Eng. Chem. 2022, 105, 63–73. DOI:10.1016/j. jiec.2021.08.017
- 22. Q. T. N. Le, E. L. Vivas, K. Cho, *J. Ind. Eng. Chem.* **2021**, 95, 57–65. **DOI:**10.1016/j.jiec.2020.12.003
- 23. A.S. Dhmees, N.M. Klaleel, S.A. Mahoud, *Egypt. J. Pet.* **2018**, 27, 1113–1121. **DOI:**10.1016/j.ejpe.2018.03.012
- T. Tsutsumi, S. Nishimoto, Y. Kameshima, M. Miyake, *J. Hazard. Mater.* 2014, 266, 174–181.
 DOI:10.1016/j.jhazmat.2013.12.024
- R.E. Kukwa, D. T. Kukwa, A. D. Oklo, T. T. Ligom, B. Ishwah, J.A. Omenka, *Am. J. Chem. Eng.* 2020, 8, 48–53.
 DOI:10.11648/j.ajche.20200802.12
- W. A. A. Sudjarwo, M. M. F. Bee, AIP Conf. Proc. 2017, 1855, 020019. DOI:10.1063/1.4985464
- F. Demir, E. M Derun, *J. Non-Cryst. Solids* 2019, 524, 119649.
 DOI:10.1016/j.jnoncrysol.2019.119649
- 28. S.S. Owoeye, F. I. Jegede, S. G. Borisade, *Mater. Chem. Phys.* **2020**,248,122915. **DOI:**10.1016/j.matchemphys.2020.122915
- Owoeye, S. S., Abegunde, S. M., Oji, B., Nano-Struct. Nano-Objects 2021, 25, 100625.
 DOI:10.1016/j.nanoso.2020.100625
- 30. A. Bilgiç, A. Çimen, *RSC Adv.* **2019**, *9*, 37403–37414. **DOI:**10.1039/C9RA05810A
- 31. Y.L. Ni'mah, A.P.K Subandi., S. Suprapto, *Heliyon* **2022**, 8, e11997. **DOI:**10.1016/j.heliyon.2022.e11997
- 32. M. Najafi, R. Rostamian, A.A. Rafati, *Chem. Eng. J.* **2011**, *168*, 426–432. **DOI:**10.1016/j.cej.2010.12.064
- 33. F. An, B. Gao, *Desalination* **2009**, 249, 1390–1396. **DOI**:10.1016/j.desal.2009.04.004
- 34. Y. Niu, R. Qu, C. Sun, C. Wang, H. Chen, C. Ji, Y. Zhang, X.

- Shao, F. Bu, *J. Hazard. Mater.* **2013**, 244–245, 276–286. **DOI**:10.1016/j.jhazmat.2012.11.042
- L. Jinrong, W. Xiaonan, L. Yao, C. Wenquan, L. Yinghua, Surf. Interfaces 2018, 12, 108–115.
 DOI:10.1016/j.surfin.2018.04.005
- 36. A. A. Basaleh, M. H. Al-Malack, T.A. Saleh, *J. Environ. Chem. Eng.* **2021**, *9*, 105126. **DOI**:10.1016/j.jece.2021.105126
- 37. S. Brunauer, P. H. Emmett, E. J. Teller, *Am. Chem. Soc.* **1938**, *60*, 309–319. **DOI:**10.1021/ja01269a023
- 38. L. Velarde, D. Nikjoo, E. Escalera, F.Akhtar, *Heliyon* **2024**, *10*, e24006. **DOI**:10.1016/j.heliyon.2024.e24006
- 39. H.A. Abdelmonem, T. F. Hassanein, H. E. Sharafeldin, H. Gomaa, A. S. A. Ahmed, A. M. Abdel-lateef, E. M. Allam, M. F. Cheira, M. E. Eissa, A. H. Tilp, Colloids Surf. A: Physicochem. Eng. Asp. 2024, 684, 133081.
 - DOI:10.1016/j.colsurfa.2023.133081
- Y. Jiang, Y. Xing, S. Liu, S. Tan, Q. Huang, X. Luo, W. Chen, Biomass Bioenergy 2023, 173, 106787.
 DOI:10.1016/j.biombioe.2023.106787
- 41. E. Siswoyo, Y. Mihara, S. Tanaka, *Appl. Clay Sci.* **2014**, *97*–*98*, 146–152. **DOI**:10.1016/j.clay.2014.05.024
- 42. N. Kataria, V.K. Garg, *Chemosphere* **2018**, *208*, 818–828. **DOI:**10.1016/j.chemosphere.2018.06.022
- S. Mustapha, M.M. Ndamitso, A.S. Abdulkareem, J.O. Tijani, A.K. Mohammed, D.T. Shuaib, *Heliyon* 2019, 5, e02923. DOI:10.1016/j.heliyon.2019.e02923
- 44. Y. Zhao, S. Yang, D. Ding, J. Chen, Y. Yang, Z. Lei, C. Feng, Z. Zhang, J. Colloid Interface Sci. 2013, 395, 198–204.
 DOI:10.1016/j.jcis.2012.12.054
- R. Foroutan, R. Mohammadi, S. Farjadfard, H. Esmaeili,
 B. Ramavandi, G.A. Sorial, *Adv. Powder Technol.* 2019, 30,
 2188–2199. DOI:10.1016/j.apt.2019.06.034
- 46. P. Simha, P. Banwasi, M. Mathew, *Procedia Eng.* **2016**, *148*, 779–786. **DOI:**10.1016/j.proeng.2016.06.557
- 47. A. Gupta, C. Balomajumder, *Appl. Water Sci.* **2017**, *7*, 4361–4374. **DOI**:10.1007/s13201-017-0582-9
- 48. V. Yogeshwaran, A. K. Priya, *Mater. Today: Proc.*, **2021**, *37*, 486–495. **DOI:**10.1016/j.matpr.2020.05.467
- 49. Z. H. Khan, M. Gao, W. Qiu, M. S. Islam, Z. Song, *Chemosphere* **2020**, *246*, 125701.
- DOI:10.1016/j.chemosphere.2019.125701 50. S. Wang, T. Terdkiatburana, M.O. Tadé, Sep. Purif. Technol.
- **2008**, *62*, 64–70. **DOI:**10.1016/j.seppur.2008.01.004 51. H. Çelebi, G. Gök, and O. Gök, *Sci. Rep.* **2020**, *10*, 1–12. **DOI:**10.1038/s41598-020-74553-4
- E. K. Toss, G. C. Feijoo, A. B. Botelho Junior, D. C. R. Espinosa, M. dos P. G. Baltazar, J. A. S. Tenório, *J. Sustain. Metall.* 2023, 9, 860–870. DOI:10.1007/s40831-023-00692-3
- R. Foroutan, M. Ahmadlouydarab, B. Ramavandi, R. Mohammadi, *J. Environ. Chem. Eng.* 2018, 6, 6049–6058.
 DOI:10.1016/j.jece.2018.09.030
- T. Shi, Z. Xie, Z. Zhu, W. Shi, Y. Liu, M. Liu, X. Mo, *Int. J. Biol. Macromol.* 2023, 195, 317–328.
 DOI:10.1016/j.ijbiomac.2021.12.039
- 55. T. Chouchane, M. Yahi, A. Boukari, A. Balaska, S. Chouchane, *J. Mater. Environ. Sci.* **2016**, *7*, 2825–2842.

- J. N. Wekoye, W.C. Wanyonyi, P. T. Wangila, M. K. Tonui, *Environ. Chem. Ecotoxicol.* 2020, 2, 24–1.
 DOI:10.1016/j.enceco.2020.01.004
- 57. T. Chouchane, S. Chouchane, A. Boukari, A. Mesalhi, J. Mater. Environ. Sci. 2015, 6, 924–941.
- M. Naushad, A. Abdullah, A. A. Al-kahtani, T. Ahamad, R. Awual, T. Tatarchuk, *J. Mol. Liq.* 2019, 296, 112075.
 DOI:10.1016/j.molliq.2019.112075
- H. Xu, Y. Li, F. Zhou, H. Su, E. Yao, J. Hu, Z. Chen, *Chem. Eng. J.* 2023, 470, 144070. DOI:10.1016/j.cej.2023.144070
- S. Jellali, E. Diamantopoulos, K. Haddad, M. Anane, W. Durner, A. Mlayah, *J. Environ. Manage.* 2016, 180, 439–449.
 DOI:10.1016/j.jenvman.2016.05.055
- 61. W.J. Weber, J.C. Morriss, *ASCE* **1963**, *89*, 31–59. **DOI:**10.1061/JSEDAI.0000430
- B. T. M. Nguyet, N. H. Nghi, N. A. Tien, D. Q. Khieu, H. D. Duc, N. V. Hung, *Acta Chim. Slov.* 2022, 69, 7567.
 DOI:10.17344/acsi.2022.7567
- S. Jiang, L. Huang, T. A. H. Nguyen, O. K. Y. Sik, V. Rudolph, H. Yang, D. Zhang, *Chemosphere* 2016, 142, 64–71.
 DOI:10.1016/j.chemosphere.2015.06.079
- X. Y. Wan, Y. Q. Zhan, Z. H. Long, G. Y. Zeng, Y. He, Chem. Eng. J, 2017, 330, 491–504. DOI:10.1016/j.cej.2017.07.178
- J-Y. Do, H. Moradi, D-S. Kim, J-K. Yang, Y-Y. Chang, S. S. Choi, *Diam. Relat. Mater* 2023, *136*, 110018.
 DOI:10.1016/j.diamond.2023.110018
- Y. Zhang, C. Hui, R. Wei, Y. Jiang, L. Xu, Y. Zhao, L. Du, H. Jiang, *Appl. Surf. Sci.* 2022, 573, 151627.
 DOI:10.1016/j.apsusc.2021.151627

- 67. C. Xiong, C. Yao, L. Wang, J, Ke, *Hydrometallurgy* **2009**, 98, 318–324. **DOI:**10.1016/j.hydromet.2009.05.008
- N. Nkosi, N. D Shooto, P. Nyamukamba, P. M. Thabede, *Energy Nexus* 2024, *15*, 100313.
 DOI:10.1016/j.nexus.2024.100313
- T. Sheela, Y. A. Nayaka, *Chem. Eng. J.* 2012, 191, 123–131.
 DOI:10.1016/j.cej.2012.02.080
- Y. Zhang, C. Hui, R. Wei, Y. Jiang, L. Xu, Y. Zhao, L. Du, H. Jiang, *Appl. Surf. Sci.* 2022, 573, 151627.
 DOI:10.1016/j.apsusc.2021.151627
- X. Y. Wan, Y. Q. Zhan, Z. H. Long, G. Y. Zeng, Y. He, Chem. Eng. J. 2017, 330, 491–504. DOI:10.1016/j.cej.2017.07.178
- A. Sarı, D. Cıtak M. Tuzen, Chem. Eng. J. 2010, 162, 521–527.
 DOI:10.1016/j.cej.2010.05.054
- M. Sh. Gohr, A. I. Abd-Elhamid, A. A. El-Shanshory, H. M. A. Soliman, *J. Mol. Liq*, 2022, 346, 118227.
 DOI:10.1016/j.molliq.2021.118227
- A. Nakhli, M. Bergaoui, C. Aguir, M. Khalfaoui, M. F. M'Henni, A.B. Lamine, *Desalination Water Treat.* 2016, 57, 12730–12742. DOI:10.1080/19443994.2015.1052564
- M. Zhang, Q. Yao, C. Lu, Z. Li, W. Wang, ACS Appl. Mater. Interfaces 2014, 6, 20225–20233. DOI:10.1021/am505765e
- I. Khoshkerdar, H. Esmaeili, Acta Chim. Slov. 2019, 66, 208– 216. DOI:10.17344/acsi.2018.4795
- E. Daneshvar, A. Vazirzadeh, A. Niazi, M. Kousha, M. Naushad, A. Bhatnagar, *J. Clean. Prod.* 2017, 152:443–453.
 DOI:10.1016/j.jclepro.2017.03.119
- 78. E. Igberase, P. Osifo, A. Ofomaja, *J. Environ. Chem. Eng.* **2014**, 2, 362–369. **DOI:**10.1016/j.jece.2014.01.008

Povzetek

V študiji je bil silikagel, pridobljen iz plavžne žlindre, uporabljen za izločanje kadmija v šaržnem načinu pod delovanjem različnih dejavnikov. Fizikalno-kemijske analize so pokazale, da je modificirana žlindra sestavljena samo iz kremena (96,14%). Njegova specifična površina je 484 m 2 g $^{-1}$ in pH, ki ustreza točki ničelnega naboja, je 4,2. Eksperiment je pokazal, da je pri pH 6 vpliv determinantnih dejavnikov prispeval k povečanju sorpcijske kapacitete, ki je bila izmerjena pri 154,11 mg/g in je bila dosežena na homogeni enoslojni površini (R2 = 099). Kinetična analiza je pokazala, da se ta proces ujema s kinetičnim modelom psevdodrugega reda (R2 \geq 0,99). Poleg tega je bilo navedeno, da je difuzija onesnaževala zagotovljena z zunanjo difuzijo in difuzijo znotraj delcev. Vrednosti termodinamskih spremenljivk so pojasnile, da je sorpcija kadmija spontana, eksotermna, z nižjo entropijo in izvedena pod vplivom elektrostatične interakcije. Postopek desorpcije je pokazal, da je bila ponovna uporaba silikagela izvedljiva v petih zaporednih ciklih.



Except when otherwise noted, articles in this journal are published under the terms and conditions of the Creative Commons Attribution 4.0 International License